Journal of Optoelectronics and Advanced Materials Vol. 6, No. 2, June 2004, p. 575 - 580

INVITED PAPER

ANALYSIS OF THE FREQUENCY DEPENDENCE OF THE MAGNETOIMPEDANCE IN CURRENT ANNEALED AMORPHOUS WIRES

V. Raposo*, D. García, O. Montero A. G. Flores, J. I. Iñiguez

Dpto. Física Aplicada, Universidad de Salamanca, Plaza de la Merced s/n, 37008 Salamanca, Spain

Magnetoimpedance in amorphous wires in their as-cast and after current annealing has been measured in the range from 0.1 to 30 MHz. In Fe rich wires there is an increase of the magnetoimpedance ratio with annealing until full crystallization of the sample. Analysis of both the hysteresis loops and the real and imaginary parts of the impedance shows the induction of circular permeability in the samples. The behavior of the impedance of the sample can be reproduced by a modified core-shell model which takes into account the magnetic losses in the wire. When plotting the phase angle of the complex impedance, the difference between the classical and modified model becomes apparent. Experimental measurements show a maximum of the phase angle caused by the combination of the existence of two different permeabilities in the core and the shell and the magnetic losses that exist within the wire. There are also other smaller peaks in the phase angle in the measured range caused by three resonances of magnetoelastic nature. Similar behavior is present in as-cast Co based wires with vanishing magnetostriction which presents very high values of the circular permeability in the external shell but no resonant peaks.

(Received April 26, 2004; accepted June 3, 2004)

Keywords: Amorphous wires, Giant magnetoimpedance, Complex impedance phase angle, Permeability, Magnetic losses, Resonance

1. Introduction

Magnetoimpedance (MI), discovered some years ago in amorphous samples, has generated growing interest because of their promising applications in magnetic sensors [1-8]. The MI effect originates in the skin effect as a consequence of the changes in the penetration depth induced by the static external field through a modification of the transverse susceptibility [9]. When the frequency is high enough the skin effect plays an important role reducing the effective section of the sample and then increasing the impedance. The change of impedance is a consequence of the modification of the skin depth with that external field and is given by:

$$\delta = \sqrt{\frac{\rho}{\pi f \mu}}, \tag{1}$$

where f is the ac current frequency, ρ is the resistivity and μ the permeability of the material. The impedance of a wire of radius *a* and conductivity σ is then given by [9]:

$$Z(\omega) = -\sqrt{-j\omega\mu\sigma}\,\frac{J_0\left(\sqrt{-j\omega\mu\sigma}\,a\right)}{J_0'\left(\sqrt{-j\omega\mu\sigma}\,a\right)}, \tag{2}$$

where j is the imaginary unit and J_0 and J_0' are the zero order Bessel function and its derivative. The resistance and reactance corresponds to the real and imaginary parts of this expression respectively. The magnetoimpedance ratio is usually defined as:

* Corresponding author: victor@usal.es

$$MI(\%) = 100 \times \frac{Z(H) - Z(H_{max})}{Z(H_{max})}, \quad (3)$$

where H_{max} is the maximum applied field to the sample.
The study of the frequency dependence of the complex impedance of the sample will provide information about the permeability models describing the behavior of the sample as well as other contribution leading to the presence of magnetic resonances. The current annealing of wires with low initial magnetoimpedance ratio provides useful information about the induction of circular permeabilities and its influence on the impedance.

2. Experimental

$Fe_{77.5}Si_{7.5}B_{15}$ commercial amorphous wires with a diameter of 125 μm were provided by Goodfellow. $Co_{68.15}Fe_{4.35}Si_{12.5}B_{15}$, $Co_{72.5}Si_{12.5}B_{15}$ and $Fe_{73.5}Nb_3Cu_1Si_{13.5}B_9$ amorphous wires were prepared by the in-rotating-water quenching technique [10]. Cobalt 3000 samples with nearly zero magnetostriction constant and 100 μm in diameter where provided by Global Micro Wire Technologies. Pieces of about 150 mm in length were taken for the experiments.

Axial and circular hysteresis loops were measured by the conventional fluxmetric method. For GMI measurements both real and imaginary parts of the impedance of the sample were obtained using the four point technique by an LCR bride model HP 4285A from Agilent Technologies. A schematic setup is presented in Fig. 1. The frequency dependence was studied in the range from 75 kHz to 30 MHz while the AC current was maintained constant at 1 mA. The magnetic field was generated by a pair of Helmholtz coils connected to a programmable bipolar power supply from Kepco which produces a maximum field of 15 kA/m. The system was placed inside a magnetic screening to avoid the influence of any external field.

To study the temperature dependence of the magnetoimpedance the sample was placed inside a cryostat and the impedance was measured by a lock-in amplifier in the low frequency range. For the current treatments the sample was placed in a furnace in helium atmosphere to avoid oxidation. The wire was connected to a DC current source during the desired treatment time and then cooled in the furnace before extracting the sample.

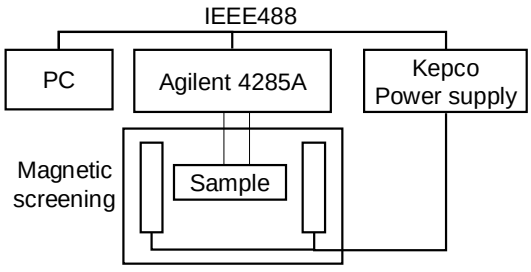

Fig. 1. Diagram block of the measuring set-up.

3. Results

Fig. 2 shows the magnetoimpedance ratio obtained from (3) as well as the corresponding magnetoresistance and magnetoinductance obtained from the real and imaginary parts of the complex impedance respectively for different wires. For the low frequency range the changes of the permeability are directly reflected in the inductance ($L = \mu/8\pi$) and the percent change on it becomes very high while the changes in the resistance are smaller due to the smaller influence of the skin effect. At high frequencies the skin effect plays an important role and the changes of the resistance growth up to 800 % while the changes in the inductance decreases. The global effect on the impedance is compensated and the magnetoimpendance ratio is maintained nearly constant up to 30 MHz with a smooth peak at intermediate frequencies.

As was expected the MI ratio is not very high for Fe-rich samples which present radial permeability, while the Co based samples with circular permeability exhibit higher MI ratios. Also Fe based wires with higher magnetostriction constant, have some peaks due to the appearance of resonances. The typical shapes of the MI for the previous wires at a fixed frequency are presented in Fig. 3. Cobalt based wires presents double peak structure in the MI but Fe based samples present single peak.

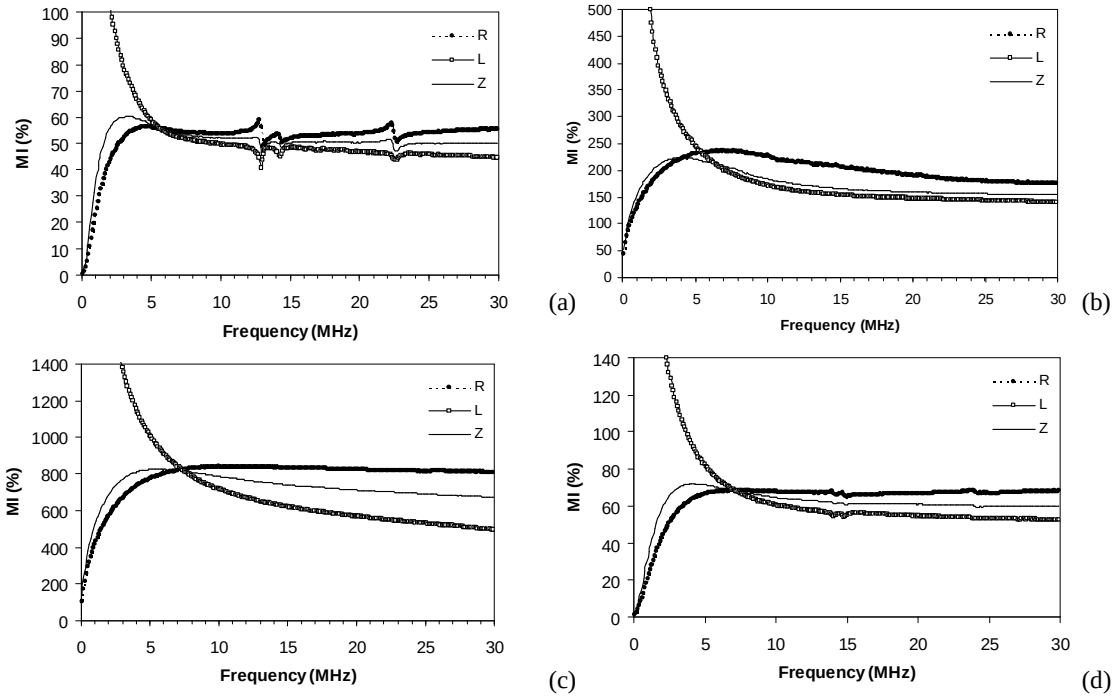

Fig. 2. Magnetoimpedance, magnetoresistance and magnetoinductance of FeSiB(a), CoSiB(b), CoFeSiB(c), and FeNbCuSiB(d) amorphous wires.

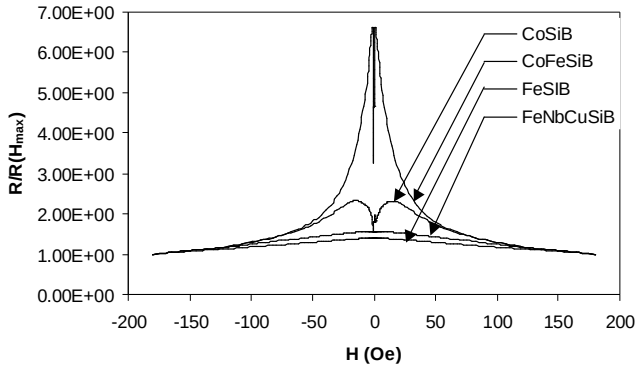

Fig. 3. Magnetoimpedance at 5 MHz for the different wires.

The behaviour of these wires is usually described by a core-shell model [11] with two different permeabilities. In the case of Co based wires the differences in the circular permeability for the core and the shell is very high, but for Fe based wires the values are not very different and they behave quite similar to equation (3). In order to increase the differences between the core an the shell the FeSiB wire was submitted to different current annealing treatment to induce circular permeability in the external shell. The influence on the MI ratio is clear as plotted in Fig. 4. MI ratio initially increases with current density and treatment time until the crystallization of the sample starts to devitrify the sample. At this point increasing the treatment time leads to a decrease of the MI ratio and crystallization of the sample until it looses the amorphous structure as revealed by the hysteresis loops.

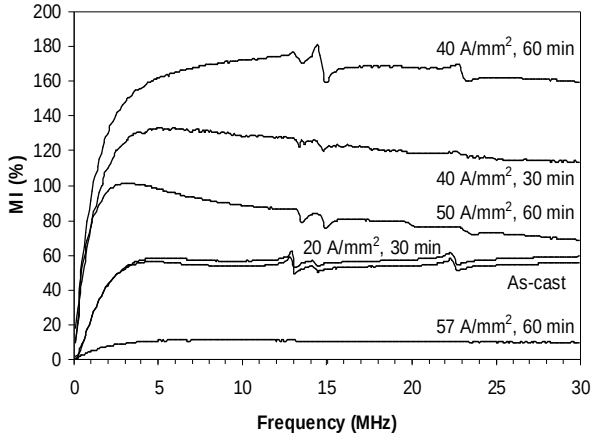

Fig. 4. Comparison of the MI ratio for the FeSiB after different current annealing treatments.

4. Discussion

In order to describe the behavior of the FeSiB sample core shell model has to be considered [11]. The impedance of a wire of radius r_0 with a core of radius r_b, and conductivity σ is obtained from:

$$\overline{Z} = \frac{lk_s}{2\pi\sigma r_0 D'}\left[A_2' J_0(k_s r_0) + B_2' Y_0(k_s r_0)\right] \tag{4}$$

where the constants are given by:

$$A_2' = k_s J_1(k_c r_b) Y_0(k_s r_b) - Y_1(k_s r_b)[k_c J_0(k_c r_b)]$$
$$B_2' = J_1(k_s r_b)[k_c J_0(k_c r_b)] - k_s J_1(k_c r_b) J_0(k_s r_b)$$
$$D' = [k_c J_0(k_c r_b)][J_1(k_s r_b) Y_1(k_s r_0) - Y_1(k_s r_b) J_1(k_s r_0)] +$$
$$k_s J_1(k_c r_b)[Y_0(k_s r_b) J1(k_s r_0) - J_0(k_s r_b) Y_1(k_s r_0)]$$

with $k_{c,s} = \sqrt{-j\sigma\mu_{c,s}\omega}$ and $\mu_{c,s}$ the magnetic permeabilities of the core and the outer shell respectively. In order to simplify the plots and to show the real and imaginary parts of the complex impedance we will plot the phase angle of the impedance which contains information from both components and is shown to be very sensitive parameter to demonstrate the accuracy of the model [12].

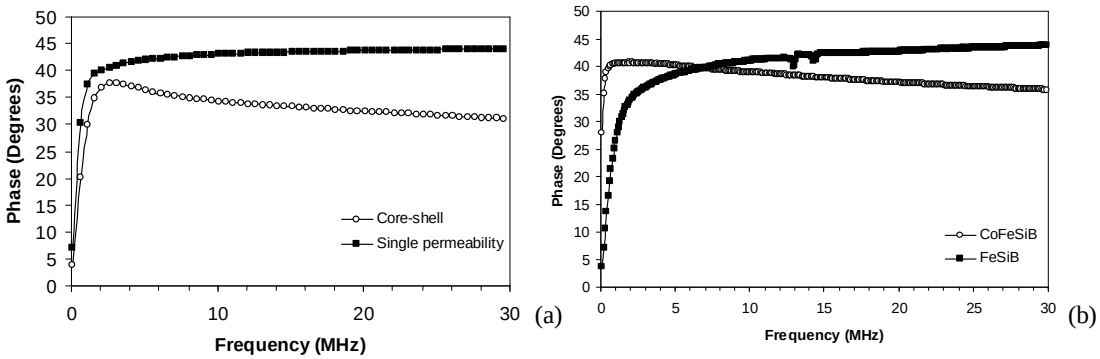

Fig. 5. Frequency dependence of the phase angle for the core-shell and classical model (a) and experimental values for CoFeSiB and FeSiB wires (b).

When using a core shell model the first difference in the phase angle is the possibility of the appearance of a peak in the phase angle at intermediate frequencies and then the asymptotical approach to 45 degrees as in the single permeability model [9]. To achieve this shape it is necessary to choose adequate values of core and shell permeability values. A monotonic increase of the phase

angle is found in the as cast sample corresponding to the single permeability model, when comparing to the experimental results. The wires presenting higher MI ratios and therefore higher circular permeabilities exhibit a decrease of the phase angle at high frequencies after a maximum close to 4 MHZ. This behavior can be reproduced including an additional term in the permeability that reflects the losses of the circular hysteresis loops by considering a complex permeabilily ($\mu = \mu' - j\,\mu''$). The introduction of the imaginary part of the permeability represents the losses of the ac hysteresis loop leading to an additional term in the resistance proportional to $\omega\mu''$ [14] that reduces the phase angle as presented in Figs. 5a and 5b.

It is clear that wires with circular permeability present a reduction of the phase angle at high frequencies caused by the magnetic losses but the Fe-rich samples behave like the classical or core-shell model without the introduction of magnetic losses.

When FeSiB samples are submitted to current annealing the increase of the MI ratio shown in Fig. 4 caused by the induction of circular permeability also reflects in the phase behavior. The as cast or devitrified wires presents low MI ratio and lower circular permeabilities and the phase angle goes asymptotically to 45º, while the samples with highest MI ratio presents a decrease of the phase caused by the magnetic looses (Fig. 6). This is also confirmed by the shape of the circular hysteresis loops (Fig. 7).

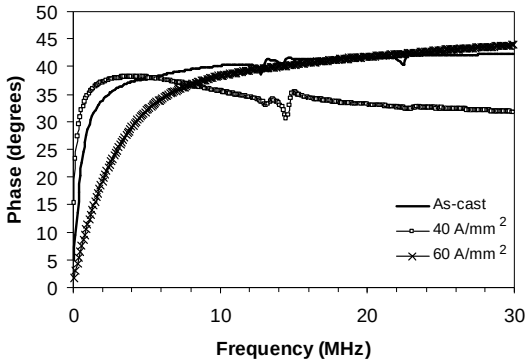

Fig. 6. Frequency dependence of the phase angle for as-cast and annealed FeSiB wires.

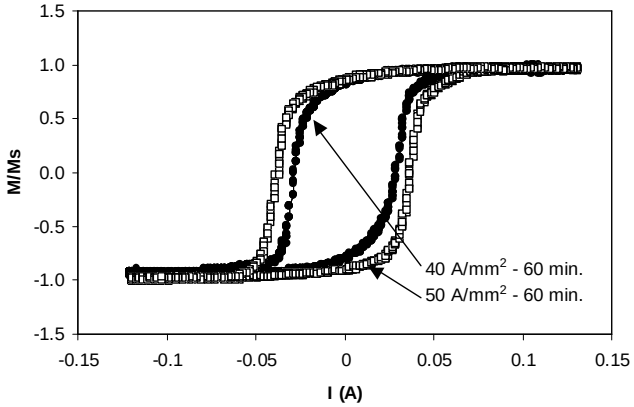

Fig. 7. Circular hysteresis loops for annealed FeSiB samples.

The presence of some peaks in both phase angle and MI ratio in FeSiB samples is due to the presence of magnetoelastic resonance. As-cast FeSiB wires have a magnetostriction constant of 30×10^{-6}. The ac current produces the circular magnetic field and in the external surface of the wire this leads to a resonant frequency [13] of:

$$f = \frac{n}{2\pi r}\sqrt{\frac{E}{\rho}} \tag{5}$$

where E represents the Young's modulus, ρ the density, r the radius of the wire and n being integer. The value for the first harmonic is 10.7 MHz, very close to the experimental one. Therefore the most

probable cause of the resonance is the waves propagating in the surface of the wire induced by the ac current.

5. Conclusions

The MI behavior of amorphous wires can be described with a core-shell model that includes the magnetic losses for wires which exhibit high circular permeability. The phase angle of the complex magnetoimpedance asymptotically reaches 45º at high frequencies for wires with low losses and these values is severely reduced in wires with circular bistability. The current annealing in FeSiB induces circular bistability and lead to higher MI ratio until crystallization of the sample that destroys the soft behaviour of the sample. The presence of peaks in the frequency dependence of the MI ratio and the phase angle are due to the existence of magnetoelastic resonance.

Acknowledgements

This work was supported in part by the MCyT of Spain under project MAT2001-0082-C04-03 and by the Junta de Castilla y León under project SA010/03.

References

[1] K. Mohri, T. Kohzawa, K. Kawashima, H. Yoshida, L. V. Panina, IEEE Trans. Magn. **28**, 3150 (1992).
[2] R. S. Beach, A. E. Berkowitz, Appl. Phys. Lett. **64**, 3652 (1994).
[3] J. Velázquez, M. Vázquez, D.-X. Chen, A. Hernando, Phys. Rev. B **50**, 16737 (1994).
[4] K. V. Rao, F. B. Humphrey, J. L. Costa-Kramer, J. Appl. Phys. **76**, 6204 (1994).
[5] L. V. Panina, K. Mohri, K. Bushida, M. D. Noda, J. Appl. Phys. **76**, 6198 (1994).
[6] R. L. Sommer, C. L. Chien, J. Appl. Phys. **79**, 5139 (1996).
[7] M. Vázquez, J. Magn. Magn. Mater. **226-230**, 693 (2001).
[8] K. Mohri, T. Uchiyama, L.P. Shen, C.M. Cai and L.V. Panina, Sensors and Actuators **A91**, 85 (2001).
[9] B. D. Popovic, "Introductory Engineering Electromagnetics", Addison Wesley (1971).
[10] I. Ogasawara, S. Ueno, IEEE Trans. Magn. **31**, 1219, (1995).
[11] D.-X. Chen, L. Pascual, E. Fraga, M. Vázquez, A. Hernando, J. Mag. Magn. Mater. **202**, 385 (1999).
[12] V. Raposo, D. García, M. Zazo, A. G. Flores, J. I Iñiguez, J. Magn. Magn. Mater., in press.
[13] B. D. Cullity, "Introduction to Magnetic Materials", Addison Wesley (1972).
[14] B. D. Popovic, "Introductory Engineering Electromagnetics" Addison Wesley (1971).